chemistry proceedings

MDPI

Proceedings

Synthesis of Conjugated Polymer Based in Zn(II) Porphyrin Bearing Terminal Alkynyl Groups as Photosensitizer †

Sofía C. Santamarina, Daniel A. Heredia, Andrés M. Durantini and Edgardo N. Durantini *

IDAS-CONICET, Departamento de Química, Facultad de Ciencias Exactas, Físico-Químicas y Naturales, Universidad Nacional de Río Cuarto, Ruta Nacional 36 Km 601, X5804BYA Río Cuarto, Córdoba, Argentina

* Correspondence: edurantini@exa.unrc.edu.ar; Tel.: +54-358-4676157

† Presented at the 24th International Electronic Conference on Synthetic Organic Chemistry, 15 November–15 December 2020; Available online: https://ecsoc-24.sciforum.net/.

Received: date; Accepted: date; Published: date

Abstract: 5,10,15,20-tetrakis-[4-(ethynyl)phenyl]porphyrin (TEP) was synthesized from the condensation of 4-(ethynyl)benzaldehyde and pyrrole catalyzed by boron trifluoride diethyl etherate in dichloromethane (DCM). After oxidation with 2,3-dichloro-5,6-dicyano-1,4-benzoquinone and purification, TEP was obtained in 34% yield. This porphyrin was metaled with Zn(II) acetate in DCM/methanol to produce the complex ZnTEP in 98% yield. Homocoupling reaction of terminal alkynes of ZnTEP to diynes was used to synthesize conjugated polymer organogel (ZnTEPP). The reaction was cocatalyzed by $PdCl_2(PPh_3)_2$ and CuI in tetrahydrofuran. The solvent was evaporated to obtain xerogel and the SEM images showed microporous structure. In addition, spectroscopic and photodynamic studies of ZnTEPP indicated that the porphyrin unit retains its properties as a photosensitizer. Thus, this polymer is an interesting material with potential applications to form photoactive aseptic surfaces.

Keywords: polymer; porphyrin; alkyne; oxidative homocoupling; photosensitizer

1. Introduction

In hospitals, surfaces are one of the main components of possible reservoirs of bacteria, which can cause a notable incidence in nosocomial infections [1]. For this purpose, photodynamic inactivation (PDI) of microorganisms has been proposed to eliminate bacteria. This therapy uses a photosensitizer, visible light and oxygen to produce highly reactive oxygen species (ROS), which can react with several cell components. These molecular modifications induce a loss of biological functionality that causes cell death [2]. In most PDI studies, photosensitizers are added to a microbial suspension from a homogeneous solution. In this methodology, after PDI treatment the photosensitizer remains in the place of action, producing an undesired photodynamic effect and contaminating the medium. In addition, under these conditions the photodynamic agent is difficult to recover for its reuse in subsequent applications. This drawback can be avoided by using photosensitizers chemically bound to a support [3]. Thus, porphyrins immobilized on a surface have been proposed for the inactivation of microorganisms, considering economic and ecological subjects. In this sense, the coating of surfaces with photosensitizers (PSs) that are immobilized in a film are of great interest to maintain aseptic surfaces in public health [4].

In this study, 5,10,15,20-tetrakis-[4-(ethynyl)phenyl]porphyrin (TEP) was synthesized by acid catalyzed condensation of 4-(ethynyl)benzaldehyde and pyrrole. This porphyrin was treated with Zn(II) to form the complex ZnTEP. Homocoupling reaction of terminal alkynes of ZnTEP to diynes was used to obtain the conjugated polymer organogel (ZnTEPP). After evaporation of the solvent, xerogel was obtained, which is a type of solid-formed gel that has a microporous structure and larger

surface area together with very smaller pore sizes. Moreover, spectroscopic and photodynamic studies of ZnTEPP indicated that the porphyrin unit retains its properties as PS. Thus, this polymer is an interesting material with potential applications to form photoactive aseptic surfaces.

2. Materials and Methods

2.1. Materials

Chemicals were obtained from Sigma-Aldrich (Milwaukee, WI, USA). They were used without further purification. Tryptic soy (TS) broth and agar from Britania (Buenos Aires, Argentina) were used in microbial cultures. Microtiter plates (96-well) were acquired to Deltalab (Barcelona, Spain). Organic solvents (GR grade) from Merck (Darmstadt, Germany) were distilled and maintained on molecular sieves. Ultrapure water was obtained from a Labconco (Kansas, MO, USA) equipment model 90901-01.

2.2. Instrumentation

Proton nuclear magnetic resonance spectra were achieved on a FT-NMR Bruker Avance DPX400 spectrometer (Bruker BioSpin, Rheinstetten, Deutschland). Mass spectra were attained on a Bruker micrO-TOF-QII (Bruker Daltonics, MA, USA) equipped with an ESI source (ESI-MS). Scanning electron microscopy (SEM) images were obtained with a field emission scanning electron microscope FE-SEM (Σigma Zeiss, Oberkochen, Germany) with a thin Cr film on the sample surface and an acceleration voltage of 5 kV. UV-visible absorption spectra were recorded on a Shimadzu UV-2401PC spectrometer (Shimadzu Corporation, Tokyo, Japan), while fluorescence spectra were carried out on a Spex FluoroMax spectrofluorometer (Horiba Jobin Yvon Inc, Edison, NJ, USA). Fluence rates were obtained with a Radiometer Laser Mate-Q (Coherent, Santa Clara, CA, USA). Photooxidation of anthracene derivative was performed with a Cole-Parmer illuminator 41720-series (Cole-Parmer, Vernon Hills, IL, USA) with a 150 W halogen lamp. Optical filter (GG455 cutoff filter) were used to select a wavelength range between 455 and 800 nm (44 mW/cm^2).

2.3. Synthesis

5,10,15,20-Tetrakis(*p*-ethynylphenyl)porphyrin (TEP). To a solution of 4-(ethinyl)benzaldehyde (260 mg, 2.0 mmol) and pyrrole (140 μL, 2.0 mmol) in 350 mL of dichloromethane (DCM) was added 70 μL of $BF_3{\cdot}OEt_2$. The reaction mixture was stirred at room temperature. After 3 h, 2,3-dichloro-5,6-dicyano-1,4-benzoquinone (DDQ, 340 mg, 1.5 mmol) was added and the mixture was stirred for 1 h under reflux. The solvent was evaporated under reduced pressure and the residue was purified by flash column chromatography (silica gel, *n*-hexane/DCM (7:3)) to yield 121 mg (34%) of TEP. ^{1}HNMR ($CDCl_3$, TMS) δ (ppm) −2.80 (brs, 2H, pyrrole NH), 3.37 (s, 4H, C≡CH,), 7.94 (d, 8H, J = 8.00 Hz, 3,5-ArH,), 8.19 (d, 8H, J = 8.00 Hz, 2,6-ArH), 8.88 (s, brs, pyrrole-H, 8H). ESI-MS (*m*/*z*) 711.2556 $[M+H]^+$ (711.2549 calculated for $C_{52}H_{30}N_4$ + H).

Zn(II) 5,10,15,20-tetrakis(*p*-ethynylphenyl)porphyrin (ZnTEP). TEP (30 mg, 0.042 mmol) was dissolved in 10 mL of DCM. Then, 5 mL of a saturated solution of Zn(II) acetate in methanol was added. The mixture was stirred for 2 h under argon at room temperature. The organic phase was washed three times with 15 mL of water. The organic solvent was evaporated under reduced pressure to obtain 32 mg (98%) of ZnTCP. ^{1}HNMR ($CDCl_3$, TMS) δ (ppm) 3.39 (s, 4H, C≡CH,), 7.92 (d, 8H, J = 8.00 Hz, 3.5-ArH,), 8.18 (d, 8H, J = 8.00Hz, 2,6-ArH), 8.84 (s, brs, pyrrole-H, 8H). ESI-MS (*m*/*z*) 773.1693 $[M+H]^+$ (773.1684 calculated for $C_{52}H_{28}N_4Zn$ + H).

Zn(II) 5,10,15,20-tetrakis(*p*-ethynylphenyl)porphyrin polymer (ZnTEPP). A sample of ZnTEP (20 mg, 0.026 mmol) was suspended in 1.1 mL of anhydrous tetrahydrofuran (THF). Then, 2 mg of $PdCl_2(PPh_3)_2$ (0.3 μmol) and 1 mg of CuI (5 μmol) were added to this solution. After these, compounds were dissolved by sonication and 21 μL of TEA was added to start the reaction. The solution was kept without stirring under nitrogen atmosphere in dark at room temperature for 48 h. Then, the polymer obtained was washed in 10 mL of THF to remove the reaction residues and the ZnTEP

monomers that did not polymerize. A portion of organogel (10 mg) was dried under vacuum to form xerogel.

2.4. Spectroscopic Studies

UV-visible absorption and fluorescence emission measurements in *N*,*N*-dimethylformamide (DMF) were achieved as previously described [**Error! Bookmark not defined.**]. Fluorescence emission spectra were recorded by exciting the samples at λ_{exc} = 550 nm. The fluorescence quantum yield (Φ_F) of each porphyrin was calculated using Zn(II) 5,10,15,20-tetrakis(4-methoxyphenyl)porphyrin (ZnTMP) as a reference (Φ_F = 0.049) in DMF [5].

2.5. Determination of $O_2(^1\Delta_g)$ Production

9,10-Dimethylanthracene (DMA, 35 μM) and the photosensitizer in DMF (2 mL) were irradiated with light at 455–800 nm. The kinetics of DMA photooxidation were analyzed by the decrease in the absorption band at λ_{max} = 378 nm. The observed rate constants k_{obs}^{DMA} of DMA oxidation and quantum yields of $O_2(^1\Delta_g)$ production (Φ_Δ) of the porphyrins were obtained as previously reported [**Error! Bookmark not defined.**]. ZnTMP was used as a reference (Φ_Δ = 0.73) [**Error! Bookmark not defined.**].

3. Results and Discussion

3.1. Synthesis of Porphyrins and Polymer

The synthetic procedure to obtain porphyrins are shown in Scheme 1. TEP was synthesized from the condensation of 4-(ethynyl)benzaldehyde and pyrrole catalyzed by $BF_3{\cdot}OEt_2$ in DCM. After oxidation with DDQ and purification by flash column chromatography (silica gel), TEP was obtained in 38% yield. This is an appropriated yield for the synthesis of symmetrically substituted porphyrin derivatives [6]. Then, TEP was metaled with Zn(II) acetate in DCM/methanol to produce the complex ZnTEP in 98% yield. This porphyrin bears four ethynylphenyl substituents at the *meso* position. Homocoupling reaction of terminal alkynes of ZnTEP to diynes was used to synthesize conjugated polymer organogel ZnTEPP (Scheme 2). The reaction was cocatalyzed by $PdCl_2(PPh_3)_2$ and CuI in THF. The polymer was washed with THF to obtain the organogel ZnTEPP. The solvent contained in this polymer was evaporated to obtain xerogel [7].

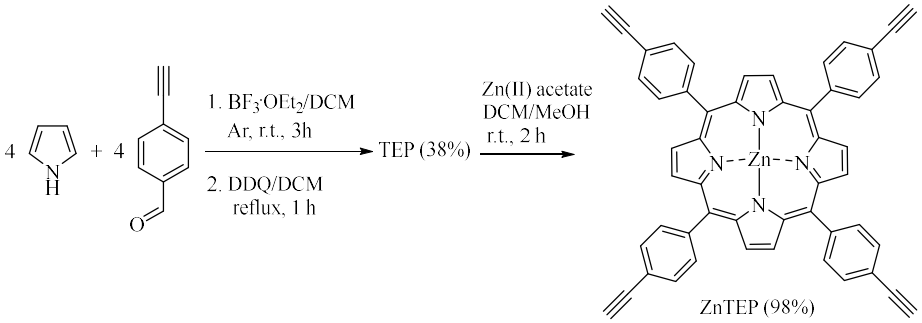

Scheme 1. Synthesis of TEP and ZnTEP.

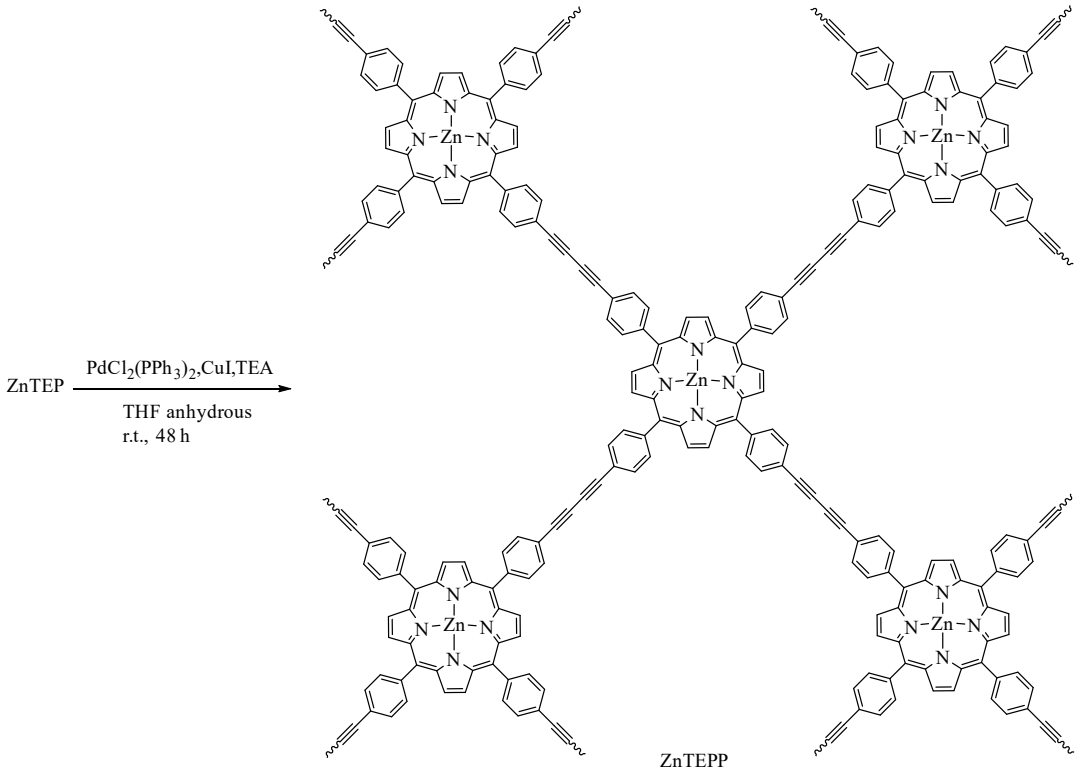

Scheme 2. Synthesis of ZnTEPP.

3.2. SEM Images

Error! Reference source not found. shows the SEM images of the ZnTEPP polymer. First, an aliquot of the organogel polymer was deposited on a glass surface as a film and the solvent was evaporated at room temperature. Images of this material are illustrated in **Error! Reference source not found.**A. As can be seen, SEM image shows a structure of superimposed scales that cover the surface. On the other hand, a representative SEM image of a portion xerogel polymer is shown in **Error! Reference source not found.**B. The porous structures are observed in the xerogel due to the removal of the solvent THF captured in the interstices of the organogel. Therefore, the xerogel can retain the original shape but with a very contracted size.

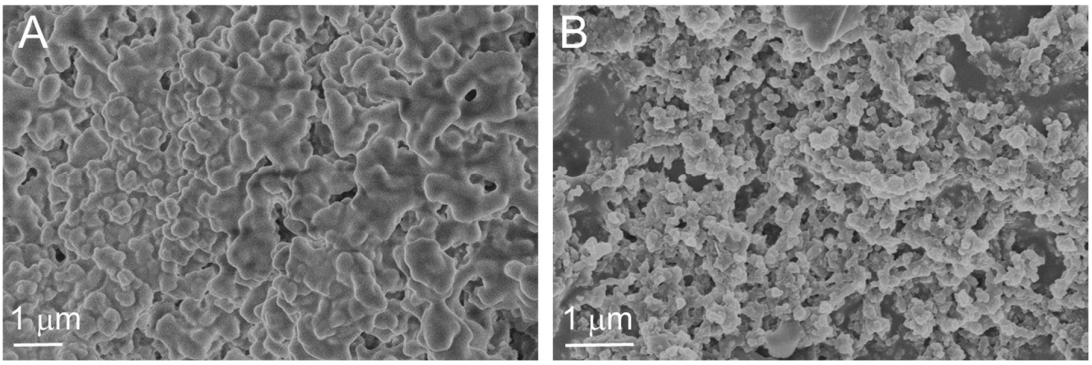

Figure 1. SEM images of ZnTEPP polymer (**A**) ZnTEPP organogel deposited as a film on glass and (**B**) a portion of ZnTEPP xerogel.

3.3. Photophysical Characterization

The UV-visible absorption spectra of ZnTEPP and its constitutional porphyrin ZnTEPP in DMF are shown in **Error! Reference source not found.**(A). These spectra were also compared with that for ZnTMP, which was used as a reference. The main optical characteristics of these compounds are summarized in **Error! Reference source not found.**. The spectra of ZnTEP and ZnTMP show the typical Soret band around 420 nm and Q-bands in the 500–600 nm range, characteristic of the corresponding Zn(II) substituted porphyrins [8]. The sharp absorption of Soret bands indicated that porphyrins are dissolved as monomer in this medium. Furthermore, the polymer ZnTEPP essentially retained the spectroscopic properties of the porphyrin-based chromophore despite to be an extensively aggregated system. The UV-visible absorption observations also confirm the polymerization of ZnTEP. The Soret and Q bands of ZnTEPP exhibit a red-shifted maximum of around 18 nm in comparison with those of ZnTEP in DMF, together with a small broadening of both bands. These results indicate only slight interaction between the porphyrin units in the polymer structure [**Error! Bookmark not defined.**].

Fluorescence emission properties of ZnTEP and ZnTMP were compared in DMF as indicated in **Error! Reference source not found.**(B). The spectra show two bands around 610 and 670 nm, which are typical for similar *meso*-substituted Zn(II) porphyrin derivatives [**Error! Bookmark not defined.**,**Error! Bookmark not defined.**]. These emission bands have been assigned to Q_x(0-0) and Q_x(0-1) transitions. This is characteristic of porphyrins with D_{2h} symmetry, indicating that the vibronic structure of the tetrapyrrolic macrocycle remains practically unchanged upon excitation [9]. The emission spectrum of ZnTEPP is characterized by a broad emission band centered at 620 nm and a second band at 680 nm. Both bands are red-shifted with respect to the monomer in solution, in agreement with the fact that the Q bands in the film are also red-shifted. In addition, ZnTEPP presented good emission proprieties indicating that the spectroscopic characteristics of the porphyrin based-chromophore were retained in the polymeric matrix. These results also indicate that the porphyrin can be embedded in the polymer without substantial aggregation. These minor spectral changes in absorbance spectrum and the fluoresce properties of the polymer suggest that the π-π stacking between the porphyrin cores is impede and only takes place a weak interaction. The fluorescence quantum yields (Φ_F) of the porphyrins were determined using ZnTMP as a reference (**Error! Reference source not found.**). The values of Φ_F for ZnTEP and ZnTEPP agree with those previously reported for similar structures [**Error! Bookmark not defined.**,**Error! Bookmark not defined.**].

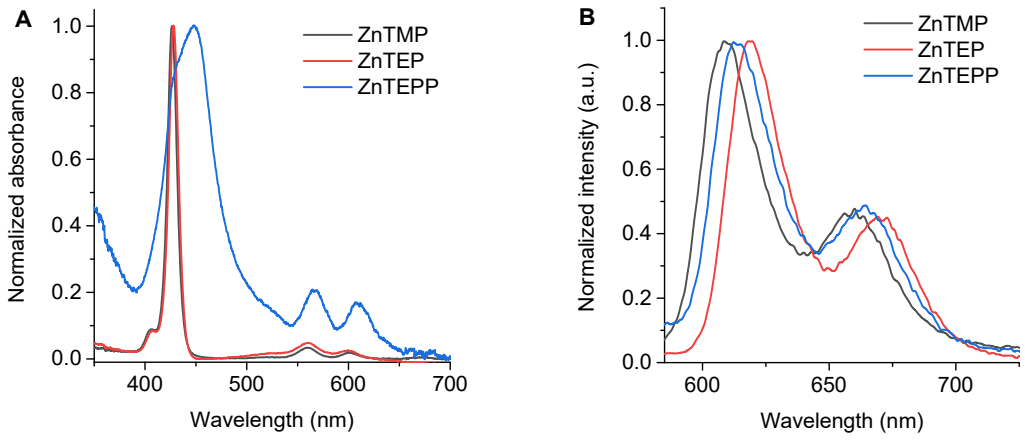

Figure 2. (**A**) UV-visible absorption spectra and (**B**) fluorescence emission spectra of ZnTMP, ZnTEP and ZnTEPP in DMF, λ_{exc} = 550 nm.

3.4. Photodynamic Properties

Photooxidation of DMA induced by ZnTEP and ZnTEPP was determined in DMF. The reaction was followed by the decay of the DMA band at 378 nm due to the formation of the 9,10-endoperoxide product [**Error! Bookmark not defined.**,**Error! Bookmark not defined.**]. Since DMA quenches $O_2(^1\Delta_g)$ by chemical reaction, it was used as an approach to determine the ability of these PSs to produce $O_2(^1\Delta_g)$ [10]. The values of k_{obs}^{DMA} were calculated from first-order kinetic plots of the DMA absorption vs. time. Also, the results were compared with those using ZnTMP as a reference. **Error! Reference source not found.** summarized the values of k_{obs}^{DMA} calculated from the first order kinetic plots. The value of k_{obs}^{DMA} for the reaction sensitized by ZnTEP is lower than that obtained for ZnTMP. In addition, the values of Φ_Δ were determined comparing the kinetic data with that of the reference. The Φ_Δ value obtained for ZnTEP was slight lower than the expected for a Zn(II) porphyrin derivative [**Error! Bookmark not defined.**]. ZnTEP is a low polar porphyrin and this tetrapyrrolic macrocycle can be not completely dissolved as a monomer in DMF, reducing the production of $O_2(^1\Delta_g)$. Photooxidation induced by ZnTEPP can be considered appropriate since $O_2(^1\Delta_g)$ generation occurs in the polymeric structure.

Table 1. Spectroscopic and photodynamic properties of ZnTMP, ZnTEP and ZnTEPP in DMF.

PS	λ^{Soret} (nm)	ε^{Soret} [a]	λ_{em}(nm)	Φ_F [b]	k_{obs}^{DMA} (s^{-1}) [c]	Φ_Δ [d]
ZnTMP	426	4.07×10^5	608	0.049 ± 0.004	$(2.02 \pm 0.02) \times 10^{-2}$	0.73 ± 0.03 [e]
ZnTEP	428	5.56×10^5	612	0.030 ± 0.003	$(1.60 \pm 0.02) \times 10^{-2}$	0.57 ± 0.03
ZnTEPP	446	-	620	0.008 ± 0.002	$(0.53 \pm 0.01) \times 10^{-4}$	0.019 ± 0.004

[a] molar absorption coefficient ($Lmol^{-1}cm^{-1}$), [b] fluorescence quantum yield, [c] observed rate constants for the photooxidation reaction of DMA, [d] quantum yield of $O_2(^1\Delta_g)$ production, [e] from Ref. [**Error! Bookmark not defined.**]. Values represent the mean ± standard deviation of three separate experiments.

4. Conclusions

The symmetrically meso substituted porphyrin TEP was synthesized from the condensation of 4-(ethynyl)benzaldehyde and pyrrole catalyzed by acid in good yield. This porphyrin was metaled with Zn(II) acetate to form the complex ZnTEP. Homocoupling reaction of terminal alkynes of ZnTEP to diynes was used to synthesize conjugated polymer organogel ZnTEPP. Moreover, the solvent was removed to obtain xerogel. SEM images of ZnTEPP showed microporous structures. The ZnTEPP polymer retains the spectroscopic characteristics of the porphyrin-based chromophore despite to be an extensively polymeric system. In addition, photodynamic studies indicated that the porphyrin unit in ZnTEPP retains its properties as PS, which was able to produce $O_2(^1\Delta_g)$. Thus, this polymer is an interesting material with potential applications to form photoactive aseptic surfaces.

Acknowledgments: This work was supported by CONICET, PIP-2015 1122015 0100197 CO, UNRC-SECYT, PPI-2020 and ANPCYT, PICT 0667/16. D.A.H, A.M.D. and E.N.D. are Scientific Members of CONICET. S.C.S. thanks CONICET for the research fellowship.

Conflicts of Interest: The authors declare no conflict of interest.

References

1. Olofsson, M.; Matussek, A.; Ehricht, R.; Lindgren, P.-E.; Östgren, C.J. Differences in molecular epidemiology of staphylococcus aureus and *Escherichia coli* in nursing home residents and people in unassisted living situations. *J. Hosp. Infect.* **2019**, *101*, 76–83.
2. Durantini, A.M.; Heredia, D.A.; Durantini, J.E.; Durantini, E.N. BODIPYs to the rescue: Potential applications in photodynamic inactivation. *Eur. J. Med. Chem.* **2018**, *144*, 651–661.
3. Spagnul, C.; Turner, L.C.; Boyle, R.W. Immobilized photosensitizers for antimicrobial applications. *J. Photochem. Photobiol. B Biol.* **2015**, *150*, 11–30.

4. Heredia, D.A.; Martínez, S.R.; Durantini, A.M.; Pérez, M.E.; Mangione, M.I.; Durantini, J.E.; Gervaldo, M.A.; Otero, L.A.; Durantini, E.N. Antimicrobial photodynamic polymeric films bearing biscarbazol triphenylamine end-capped dendrimeric Zn(II) porphyrin. *ACS Appl. Mater. Interfaces* **2019**, *11*, 27574–27587.
5. Milanesio, M.E.; Alvarez, M.G.; Yslas, E.I.; Borsarelli, C.D.; Silber, J.J.; Rivarola, V.; Durantini, E.N. Photodynamic studies of metallo 5,10,15,20-tetrakis(4-methoxyphenyl)porphyrin: Photochemical characterization and biological consequences in a human carcinoma cell line. *Photochem. Photobiol.* **2001**, *74*, 14–21.
6. Lindsey, J.S. Synthetic routes to *meso*-patterned porphyrins. *Acc. Chem. Res.* **2010**, *43*, 300–311.
7. Wu, K.; Guo, J.; Wang, C. Gelation of metalloporphyrin-based conjugated microporous polymers by oxidative homocoupling of terminal alkynes. *Chem. Mater.* **2014**, *26*, 6241–6250.
8. Scalise, I.; Durantini, E.N. Photodynamic effect of metallo 5-(4-carboxyphenyl)-10,15,20-tris(4-methylphenyl)porphyrins in biomimetic aot reverse micelles containing urease, *J. Photochem. Photobiol. A Chem.* **2004**, *162*, 105–113.
9. Lopes, J. M. S.; Sampaio, R. N.; Ito, A.S.; Batista, A.A.; Machado, A.E.H.; Araujo, P.T.; BarbosaNeto, N.M. Evolution of electronic and vibronic transitions in metal(II) *meso*-tetra(4-pyridyl)porphyrins. *Biomol. Spectrosc.* **2019**, *215*, 327–333.
10. Gomes, A.; Fernandes, E.; Lima, J.L.F.C. Fluorescence probes used for detection of reactive oxygen species. *J. Biochem. Biophys. Methods* **2005**, *65*, 45–80.